



Why Do Diffusion Data not Fit the Logistic Model? A Note on Network Discreteness, Heterogeneity & Anisotropy

Dominique Raynaud

► To cite this version:

Dominique Raynaud. Why Do Diffusion Data not Fit the Logistic Model? A Note on Network Discreteness, Heterogeneity & Anisotropy. N. Memon and R. Alhadjj, eds. From Sociology to Computing in Social Networks: Theory, Foundations and Applications, Springer-Verlag, pp.81-96, 2010. <halshs-00482597>

HAL Id: halshs-00482597

<https://halshs.archives-ouvertes.fr/halshs-00482597>

Submitted on 4 Aug 2010

HAL is a multi-disciplinary open access archive for the deposit and dissemination of scientific research documents, whether they are published or not. The documents may come from teaching and research institutions in France or abroad, or from public or private research centers.

L'archive ouverte pluridisciplinaire **HAL**, est destinée au dépôt et à la diffusion de documents scientifiques de niveau recherche, publiés ou non, émanant des établissements d'enseignement et de recherche français ou étrangers, des laboratoires publics ou privés.

Why Do Diffusion Data not Fit the Logistic Model? A Note on Network Discreteness, Heterogeneity & Anisotropy

Dominique Raynaud

Abstract Diffusion of innovations and knowledge is in most cases accounted for by the logistic model. Fieldwork research however constantly report that empirical data utterly deviate from this mathematical function. This chapter scrutinizes network forcing of diffusion process. The departure of empirical data from the logistic function is explained by social network discreteness, heterogeneity and anisotropy. New indices are proposed. Results are illustrated by empirical data from an original study of knowledge diffusion in the medieval academic network.

Introduction

Diffusion of innovations is the process by which an innovation is communicated through certain channels over time among the members of a social system [27, p. 5]. Diffusion of knowledge may be defined in the same manner, replacing what should be in the previous definition. Social network analysis is in its early stages of application to diffusion issues.

Compared with other aspects of diffusion research, there have been relatively few studies of how the social or communication structure affects the diffusion and adoption of innovations in a system [27, p. 25].

So speaks Everett M. Rogers, the outstanding promoter of diffusion studies, about the way they are connected to network analysis. In the 1970's, according to a content analysis of 1,084 empirical publications, diffusion networks represented less than one percent of diffusion research. Ten years ago, a book especially dedicated to network analysis has the same diagnosis:

Dominique Raynaud
PLC, Université de Grenoble, F-38040 Grenoble Cedex 9, and GEMASS, CNRS UMR 8598 /
Université Paris Sorbonne, 54 bd Raspail, F-75000 Paris, France
e-mail: dominique.raynaud@upmf-grenoble.fr

Only few material coupling a diffusion study with network analysis is available [8, p. 189].

The authors consequently content themselves with classical studies in the field. The fact that different authors interested in the diffusion of innovations vs. network analysis have detected the same lack of research, vouches for a promising fieldwork.

1 A Brief Historical Sketch

Despite the fact that the first paper explicitly dedicated to network diffusion was written in 1979 by Everett M. Rogers [26], the concern is much more ancient. For instance, in the course of his studies on the cholera, in 1884, Etienne-Jules Marey already applied network perspective to diffusion data. He had the insight that the topology of social network determines the form of the diffusion process. Marey says: “Closed institutions: prisons, boarding schools, convents, asylums, etc., usually escape to cholera; but if it gets into, it takes a terrible toll of victims” [20, p. 670]. Cliques (i.e. closed communities) exhibit atypical behaviour: they are resistant to the disease or completely devastated by the epidemic. The “clique effect” was independently rediscovered in 1973 by Mark S. Granovetter [12]: “weak ties” favour diffusion, “strong ties” protect the members from a tentative adoption: either they all adopt, or they all reject.

The first book approaching the diffusion of innovations through network analysis came out in 1995 by a student of Rogers: Thomas W. Valente [35]. His scope was to compare three classical datasets: the adoption of tetracycline by 130 physicians of the Middle West [6]; the diffusion of innovations among 692 Brazilian farmers [28]; the diffusion of family planning in 24 Korean villages [29]. Held with fifteen years of hindsight, the book appears a little disappointing for seven chapters out of nine are in fact dedicated to apply thresholds and critical mass models to diffusion issues. Network analysis occupies thirty pages [35, p. 31-61], where classical measures of density, centrality and equivalence are processed out on the three datasets.

In the past decades, diffusion process have been simulated either within deterministic or probabilistic models [1, 19, 16, 5, 9, 17]. Researchers have explored a full range of simulations, including Monte Carlo, Ising, Potts, Krause-Hegselmann and Deffuant models [16, 10, 32, 34, 4]. However, more often than not, models presuppose the population to be homogeneous. Simulations are implemented on regular bi-dimensional lattices. Modeling rarely assumes the topology in which the diffusion occurs, and it is only in the 2000s that sociologists, economists and physicists addressed the point [7, 15, 30, 31, 18, 2]. The network-based approach of diffusion is full of consequences, some of which are still developing.

There is consequently little research on the irregularity of diffusion curves. The state-of-the-art is the following: 1/ Threshold models have relied the γ curve slope to higher or lower individual adoption thresholds [13, 14, 36]. 2/ Critical mass models have shown that, the more the early majority members have a high centrality index, the faster the critical mass is reached, and the higher is the saturation threshold [23, 35]. 3/ In a forthcoming paper, we find, with no supplementary details,

that “important consequences of this large variability [of human behaviour] are the slowing down or speed up of information” [18, p. 6].

Diffusion irregularity is not the main concern of papers in statistical physics that closely combine network analysis with diffusion processes. They consider instead: 1/ critical points for avalanches [15]; 3/ random walks, qua they provide network topology characteristics [30]; 4/ modularity-based partitioning of graphs [31]; 5/ mean-field theory applications [2]. An overview of the current research would say that diffusion is basically seen as a *means* to find network properties. Hence, the literature is still lacking for network-based studies that could answer the long-delayed question of diffusion anomalies.

2 The Logistic Function

The choice of the mathematical model accounting for diffusion depends on the empirical conditions of spreading. If the empirical process is a step-by-step diffusion through interpersonal contacts, it follows the logistic function, which was first discovered in 1838 by Pierre-François Verhulst—albeit he never used the term [38]. In the recent years, there was a propensity to emancipate from his formalism; see [5]. In the following equation, the term $e^{-\gamma t}$ is the most characteristic of the process:

$$n_t = \frac{N'}{1 + ae^{-\gamma t}} \quad (1)$$

n_t represents the cumulative number of individuals having adopted at time t ; N' the number of susceptible adopters in the given population; a is a parameter setting the number of early adopters; γ the slope of the curve at the inflection point (when $\gamma \rightarrow 0$, the curve is flat).

The bell-shaped first derivative represents the instant number of adopters at time t . The second derivative is swing-shaped. First and second derivatives respond to equations (2) and (3) respectively:

$$\frac{dn}{dt} = \frac{\gamma N' a e^{-\gamma t}}{1 + ae^{-\gamma t}} \quad (2)$$

$$\frac{d^2n}{dt^2} = \frac{\gamma^2 N' a e^{-\gamma t} (ae^{-\gamma t} - 1)}{(1 + ae^{-\gamma t})^3} \quad (3)$$

This approach provides a natural classification of adopters through diffusion-based concepts. Introducing N' in the equations, we find that—whatever be parameters a and γ —early adopters, early majority, late majority and laggards appear at exactly 0.21, 0.5 and 0.79 of the susceptible population. These values are somewhat different from those given in Rogers’ influential book [27], and afterwards endlessly repeated in the literature. According to him, early adopters, early majority,

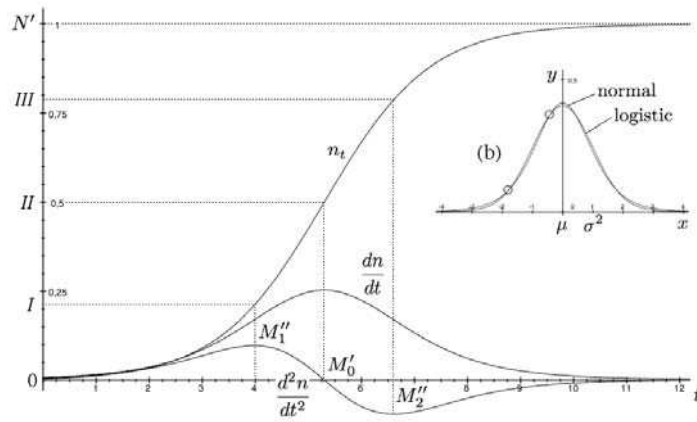


Fig. 1: The logistic function and its derivatives

late majority and laggards appear respectively at 0.16, 0.5 and 0.84 of the susceptible population.

The reason for such a disagreement is that the classification of adopters is envisaged through common statistical concepts. The logistic first derivative is assimilated to a normal distribution. Rogers' values are in fact those of the mean μ and $\mu - \sigma^2$, $\mu + \sigma^2$. Valente is even more explicit:

The logistic function has an inflexion point at 50 % adoption and two second-order inflection points, one each at one standard deviation below and above the mean [35, p. 83].

Standard deviation concept is inappropriate in this context: logistic function is not a Gaussian distribution. There is a simple visual proof for that: respective curves cross several times with each other, as in Fig. 1 (b). As a consequence, the values 0.16, 0.5 and 0.84 must be discarded and replaced by 0.21, 0.5 and 0.79.

3 Empirical Data

Does the logistic function fit the diffusion data? Compared to fieldwork data, logistic law rather appears as a mathematical ideality. In fact, curves never exhibit so a smooth and regular profile. Let us begin by the fact fieldwork studies constantly report that curves of diffusion are affected by irregularities. One can find in Valente's valuable book [35] a report on such irregularities (Fig. 2).

Such anomalies are evidently not accountable within the logistic model. We owe to Rapoport and Yuan the first penetrating remarks. While reaching the conclusion that "actual processes can be approximated by equivalent epidemics in well-mixed populations or by equivalent random social nets," they are nevertheless warning us

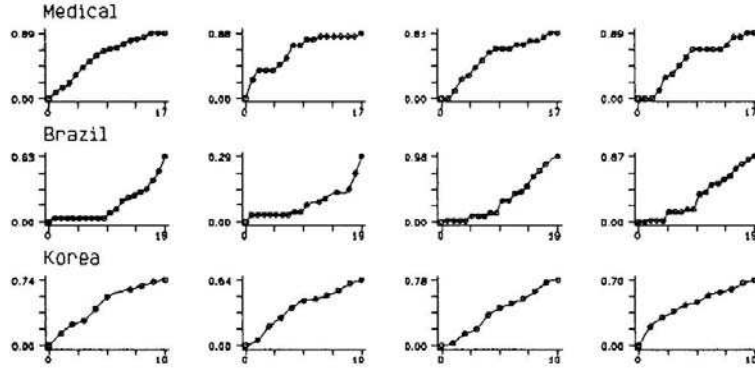


Fig. 2: Diffusion curves irregularity.

that this conjecture “does not apply to highly structured populations” [24, p. 344-345]. The gap between the model and the real world lies in the assumption that societies are “well-mixed populations,” thus assimilating the adoption of innovation to a random draw. Social network heterogeneity urges to abandon this assumption, which is the basis of all SIR—susceptible/infective/removed—epidemiological models.

During the 2000s, statistical physicists took part in the debate, by criticizing the logistic model as “utterly inaccurate” [22]. They have again argued that standard epidemiological models do not take into account that diffusions happen in highly structured, heterogeneous population, whose topology influences the very form of the diffusion [39, 21, 22]. This observation put the answer at hand.

4 Accounting for Anomalies

Let us extract empirical data from a recent study of knowledge diffusion within the academic network of medieval universities (XIIIth-XIVth centuries). In this special case, the social network is represented by a deterministic articulated k^+ -regular graph [25]. This graph $G = (V, E)$ is particularly fitted for the study of diffusion anomalies, because it is little dense: $\delta = \ell / (g(g-1)) = 0.069$ and little cohesive: $\chi = (2 \sum_{i=1}^g \sum_{j=1}^g x_{ij} / (v_i, v_j) \Rightarrow (v_j, v_i)) / (g(g-1)) = 0.047$. In the following sections, these data will be used to illustrate theoretical findings.

The deviation of diffusion curves from the logistic model appears by superimposing the curves that have any vertex of the graph as emitter (Fig. 3). Since the set is heterogeneous, we may decompose it into subsets. Let us for instance isolate all curves whose receptor belongs to component \mathcal{P}_7 (Fig. 4).

We are now in position to investigate the main causes why empirical diffusion curves deviate from the logistic function. Let us call, by license, “fast diffusion”

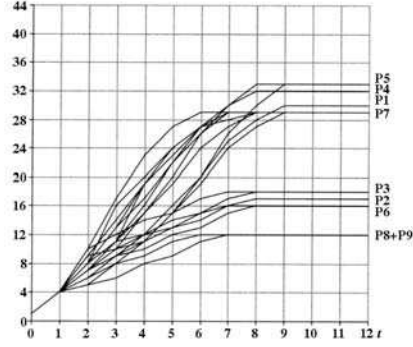
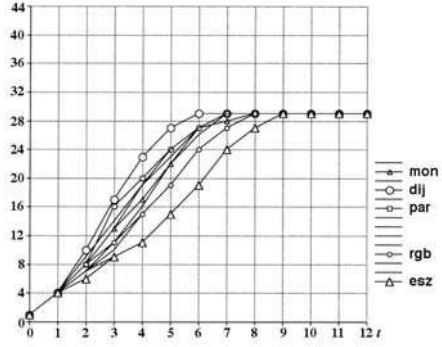


Fig. 3: Diffusion (any receptor)

Fig. 4: Diffusion (receptor $\in \mathcal{P}_7$)

any diffusion that converts many vertices in few steps; “slow diffusion” the one that either converts few vertices, or requires many steps to convert them all. Analytical concepts presented hereinafter are devised to fit diffusion networks that are always directed graphs and, more often than not, *grounded networks*—i.e. dependent on the position of vertices in space.

5 Net Discreteness

Discreteness of social networks results in slowing down/accelerating adoption, hence flattening/straightening the diffusion curve.

The more obvious difference between the logistic function (Fig. 1) and empirical curves (Fig. 3 and 4), is that the former is a smooth curve, when the latter is angled. While the logistic function is defined on a continuous (infinite) set, social diffusion happens within discrete (finite) structures. The lower the number of susceptible adopters, the more angled the curve.

There is a simple estimate for network discreteness. Let us call v_i the emitter vertex of any given diffusion process. The number of diffusion steps will be equal to the length of the longest geodesic d_{ik} originating in v_i . Local discreteness ranges from 0 when $d_{ik} = \infty$, to 1 when $d_{ik} = 1$, hence:

$$D_i = \frac{1}{\max(d_{ik})} \quad D_i \in [0, 1] \quad (4)$$

If we need a comparative index, we first calculate the mean discreteness D_G —where g is the total number of vertices—, then the difference $D'_i = D_i - D_G$:

$$D'_i = \frac{1}{\max(d_{ik})} - \frac{1}{g} \sum_{j=1}^g \frac{1}{\max(d_{jk})} \quad D'_i \in [-1, +1] \quad (5)$$

Local discreteness is null if the geodesic on which the vertex stands is as long as the graph mean geodesics. Positive values occur if $D_i \geq D_G$, when the region in which the information is going through is less dense than the rest of the graph, thus slowing down the diffusion; negative values otherwise. Discreteness values on the academic network are given in Appendix (columns D_i and D'_i). The data (ROS, 0.111, -0.048) are to be read as: “All vertices standing on the longest geodesic attached to ROS, i.e. {ROS, KOL, STR, DIJ, AST, GEN, PIS, SIE, PER, TOD, ROM} have discreteness 0.111 or, equivalently, are 0.048 less discrete than the rest of the graph.”

6 Net Heterogeneity

Heterogeneity of social networks results in slowing down/accelerating adoption, hence flattening/straightening the diffusion curve.

Let us consider anew all curves of diffusion (Fig. 4). At $t = 2$, the curves, which were hitherto undifferentiated, split into five distinct profiles. The message from DIJ is adopted by six new vertices (fast growth); the one from ESZ is adopted by only two new vertices (slow growth). This difference is due to the fact the first message is diffused within two distinct subsets, when the second message never leaves the starting subset, composed of few susceptible adopters. The diffusion growth is as fast as the conversion rate. It is only when the message gets into new components of the network that it can cause mass adoption. Consequently, slow and fast phases are sensitive to articulators.

Network forcing is detectable by visual inspection. Let us consider STR vs. FLO as emitters. Two steps after he has quitted STR, the message propagates at constant rate $e_i = 5$ (Fig. 5). In the meanwhile, after having been constant until $t = 3$, FLO message adoption rate decreases to $e_i = 0$ (Fig. 6). Vertex STR connects immediately to two components, when FLO can join few vertices only. As a result, at $t = 5$, the message has touched 24 vertices (STR) vs. 12 vertices (FLO). Network properties subtending this contrastive behaviour are: STR articulator status and low transitivity ($T = 0.166$) vs. FLO confinement and high transitivity ($T = 0.5$), that is, high vs. low area heterogeneity.

The concept of social heterogeneity has become familiar since the discovery of “structural holes” by Peter Blau [3]. Several methods exist to detect structural holes and heterogeneity in a graph [11, 33]. We can proceed with by defining local density for vertex v_i —thus adapting graph density $\delta_G = L/g(g-1)$ to a local neighbourhood. Let us first define the neighbourhood as the circle of center v_i and radius $r = \max(d_{ij})$, equal to the Euclidean distance of the remotest vertex v_j to which v_i is connected (whatever be the direction of the arc). Let ℓ_i be the outdegree of vertex v_i , and k_i the number of possible arcs capable of being built in this region. Local heterogeneity is:

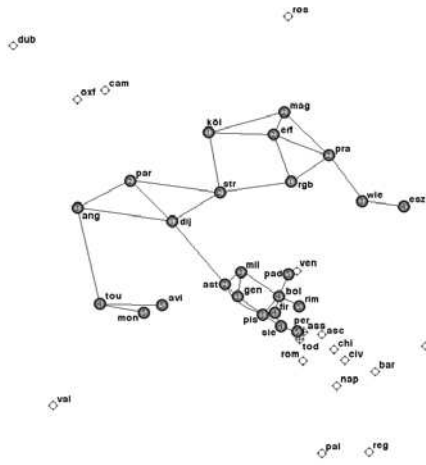


Fig. 5: Fast diffusion from STR

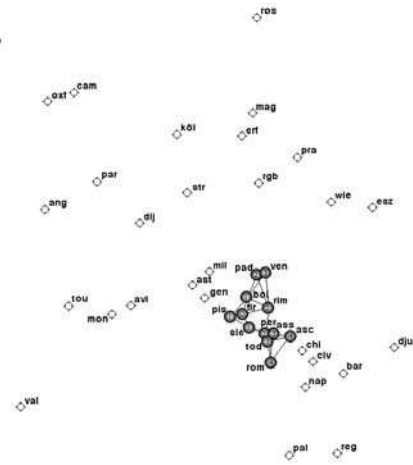


Fig. 6: Slow diffusion from FLO

$$H_i = 1 - \frac{\ell_i}{k_i} \quad H_i \in [0, 1] \quad (6)$$

If we prefer a comparative index, we first calculate the mean heterogeneity H_G on the graph, then the difference $H'_i = H_i - H_G$:

$$H'_i = \left(1 - \frac{\ell_i}{k_i}\right) - \frac{1}{g} \sum_{j=1}^g \left(1 - \frac{\ell_j}{k_j}\right) \text{ that is equal to :}$$

$$H'_i = \frac{1}{g} \sum_{j=1}^g \left(\frac{\ell_j}{k_j}\right) - \frac{\ell_i}{k_i} \quad H'_i \in [-1, +1] \quad (7)$$

This index is null when the region the information is going through is as dense as the whole graph. Positive values occur when $H_i \geq H_G$, that is when the local region is more heterogeneous than the rest of the graph, thus slowing down the diffusion; negative values otherwise. See Appendix for academic network values (columns H_i and H'_i). For example, the data (ROS, 0.000, -0.323) are to be read as: "Vertex ROS has null heterogeneity or, equivalently, is 0.323 less heterogeneous than the rest of the graph."

7 Net Anisotropy

Anisotropy of social networks results in slowing down/accelerating adoption, hence flattening/straightening the diffusion curve.

Let us isolate curves originating in DIJ and ESZ, two vertices having the greatest difference among component \mathcal{P}_7 . A good way to link irregularity of curves with network properties is to represent the message progression within the network by joining all vertices converted at the same time by “isochrones.” Fast spreading is associated to even isochrones when slow diffusion is coupled with uneven isochrones. As a result, six to nine steps are needed so that DIJ and ESZ information could cover the same area (Fig. 7 and 8). At any first steps, DIJ can distribute the message all around (quasi-isotropy), when ESZ can send information to its western neighbours only (anisotropy). This is a last factor explaining anomalies.

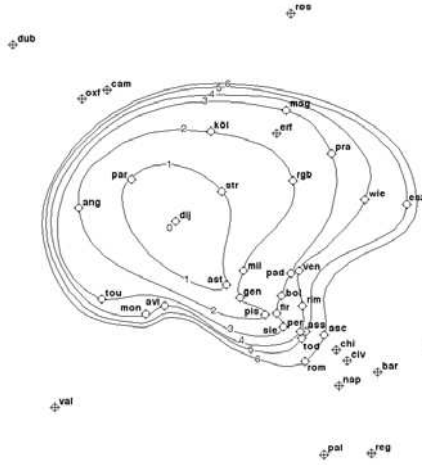


Fig. 7: Fast diffusion from DIJ

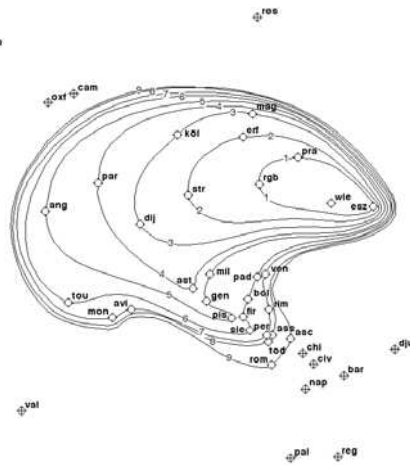


Fig. 8: Slow diffusion from ESZ

As far as I know, network anisotropy has never been defined in network analysis literature. This concept could be derived from other fields of physics, as optics, electricity or magnetism, but in the special case of grounded social networks, there is a more direct method to define the concept of anisotropy. Suppose vertex v_i has an outdegree ℓ_i and let α_{mn} be the angle of two adjacent arcs. The isotropic case arises when every angle is equal to $2\pi/\ell_i$. In order to appreciate anisotropy, we define the deviation of angle α_{mn} from $2\pi/\ell_i$. Vertex local anisotropy will then be the sum of actual deviations divided by the sum of theoretical maximum deviations:

$$A_i = \frac{\left| \alpha_{mn} - \frac{2\pi}{\ell_i} \right| + \left| \alpha_{no} - \frac{2\pi}{\ell_i} \right| + \dots + \left| \alpha_{sm} - \frac{2\pi}{\ell_i} \right|}{2(\ell_i - 1) \frac{2\pi}{\ell_i}}$$

Since angles $\alpha_{mn}, \alpha_{no} \dots$ are supplementary, we may simplify:

$$A_i = \frac{2 \max \left| \alpha_{mn} - \frac{2\pi}{\ell_i} \right|}{2(\ell_i - 1) \frac{2\pi}{\ell_i}} \quad \therefore$$

$$A_i = \frac{\ell_i \max \left| \alpha_{mn} - \frac{2\pi}{\ell_i} \right|}{2\pi(\ell_i - 1)} \quad A_i \in [0, +1] \quad (8)$$

The comparative index is obtained as previously, by calculating the mean anisotropy A_G on the graph (with g vertices), then the difference $A'_i = A_i - A_G$:

$$A'_i = \frac{1}{2\pi} \left[\frac{\ell_i \max \left| \alpha_{mn} - \frac{2\pi}{\ell_i} \right|}{(\ell_i - 1)} - \frac{1}{g} \sum_{j=1}^g \frac{\ell_j \max \left| \alpha_{pq} - \frac{2\pi}{\ell_j} \right|}{(\ell_j - 1)} \right] \quad A'_i \in [-1, +1] \quad (9)$$

Local anisotropy is null when the local region has the same degree of isotropy as the rest of the graph. Positive values occur in the case $A_i \geq A_G$, when the region the message is going through is less isotropic than the rest of the graph, thus slowing down the diffusion; negative values otherwise. See Appendix for academic network data (columns A_i and A'_i). The data (ROS, 0.866, +0.388) are to be read as: “Vertex ROS has anisotropy 0.866 or, equivalently, is 0.388 more anisotropic than the rest of the graph.”

8 A Test of DHA Indices

First of all, the definition of D (discreteness), H (heterogeneity) and A (anisotropy) enables us to tell the difference between regular and irregular graphs. In a 2D square lattice, all geodesics are infinite, the term $1/d_{ik}$ is null and $D = 0$. Since all vertices are disposed regularly, and have the same outdegree, the term $\ell_i/k_i = +1$ everywhere, thus $H = 0$. Finally, since angles of all adjacent arcs are equal, any term $\alpha_{mn} = 2\pi/\ell_i$ so that $A = 0$. We recognize a well known property: a lattice is a perfect infinite, homogeneous and isotropic network.

Social networks utterly differ from this model. Regarding the conditions of spreading in the same graph, DHA indices make it possible to see the regions where the diffusion is speeding up, and where it is slowing down. Let us resume the discussion of the medieval academic network and compare the indices of all vertices (see Appendix). Network mean values are: discreteness $D_G = 0.159$, heterogeneity $H_G = 0.323$, anisotropy $A_G = 0.478$. Because of the problem of sign combination, it is not appropriate to aggregate directly DHA indices. General results are nonetheless accessible.

Maximum discreteness occurs for vertices in the graph innermost component {AST, MIL, PAD, VEN, GEN, BOL, PIS, FIR, SIE, RIM, PER} because several directed

filters impede information to propagate outside the component, thereby reducing the number of steps of diffusion. Maximum heterogeneity occurs for vertices situated on the borders of the central component {AST, PIS, ROM, CHI, CIV} because those vertices are both in dense regions and in position to be tied to many vertices with which they have no actual relation. Maximum anisotropy occurs for the outermost vertices of the graph (DUB, ROS, ESZ, DJU) because they can send information only inwards the network.

All vertices are now sorted into eight classes, according to the sign of their indices (see Appendix, last column):

- {OXF, CAM, WIE}
- +- - {MON, AVI, GEN, FIR, PAD}
- +- {PRA, ERF, RGB, STR, PAR, VAL, ASC, CHI, CIV}
- + {LIS, SEV, SAL, TOU, ANG, DUB, ROS, ESZ, DJU, REG, PAL}
- ++- {DIJ, BOL, SIE, PER, ASS, TOD}
- + - + {MIL, VEN}
- + + {MAG, KOL, BAR, NAP}
- +++ {AST, PIS, ROM, RIM}

The behaviour of classes (---) and (+++) is quite obvious. Other classes can either accelerate or slow down the diffusion.

A 3D-plotting ($x = D, y = H, z = A$) shows the wide dispersion of vertices on both HA axes (Fig. 9), while D seems to have a much more limited impact on how they are spatially distributed (Fig. 10). This limitation is not a general property. It is due to the academic network small diameter, $\phi = 9$. I have plotted in light blue low-valued vertices, for which the corresponding vector has length $x \leq 0.300$ {MAG, ERF, PRA, TOU, VAL, BOL, SIE, PER, TOD, ASC}.

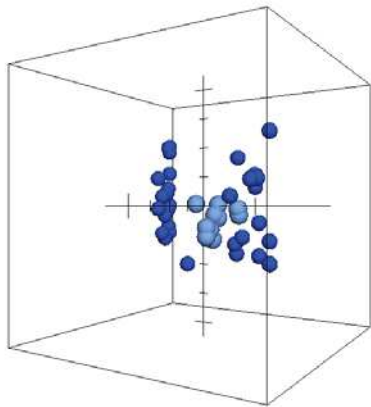


Fig. 9: DHA dispersion of vertices

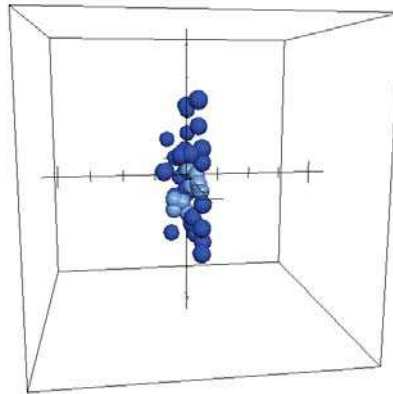


Fig. 10: D index limited impact

In DHA space, vertices that are speeding up vs. slowing down diffusion are separated by the plane Γ of equation:

$$-x - y - z = 0 \quad (10)$$

Accordingly, the impact of each node on the diffusion shape can be estimated by the Euclidean distance of any vertex v_i of coordinates (D'_i, H'_i, A'_i) to the plane Γ :

$$\omega_i = \frac{1}{\sqrt{3}} |-D'_i - H'_i - A'_i| \quad (11)$$

As a result, this compounded index (Appendix, column ω_i) tells us how much the network vertex is contributing to the deviation from the logistic curve. When ω_i sign is negative (yellow) the diffusion is accelerating, when it is positive (blue) the diffusion is slowing down (Fig. 11).

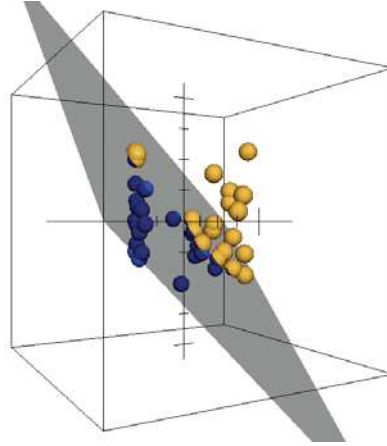


Fig. 11: DHA values

Focus now on the most contrastive classes of network vertices. Nodes which are speeding up the diffusion are in general situated in the innermost parts of the outer components {WIE, CAM, OXF, AVI, MON, SAL, SEV}. Conversely, nodes which are slowing down the diffusion are to be found in the outermost parts of the inner components {AST, PIS, RIM, CHI, ROM}; while out-out vertices {LIS, TOU, ANG, DUB, ROS, ESZ, MIL, PAD, VEN, DJU, REG, PAL} and in-in vertices {SIE, PER, ASS, TOD} have actually little impact on the diffusion.

Conclusion

We are now in position to answer the issue addressed at the beginning of the chapter: *Diffusion data do not fit the logistic model because social space is discrete, heterogeneous and anisotropic*. Social space is thus an inadequate metaphor that should be outlawed. Any social spreading of innovations and knowledge is network-dependent. The agenda for future research should plan to: 1/ test DHA indices robustness—especially the concept of “net anisotropy” presented in these pages, 2/ focus on how DHA indices could predict the precise shape of a diffusion process occurring in a given social network and, conversely, 3/ deduce, from any empirical data on social diffusion, the DHA indices of the social network in which the diffusion takes place.

Appendix: Academic Network DHA Indices

Code	University	D_i	H_i	A_i	D'_i	H'_i	A'_i	Sign	ω_i
ROS	Røskilde	0.111	0.000	0.867	-0.048	-0.323	0.389	--+	+0.010
MAG	Magdeburg	0.111	0.410	0.487	-0.048	0.087	0.009	-++	+0.028
ERF	Erfurt	0.111	0.571	0.417	-0.048	0.248	-0.061	-+-	+0.080
PRA	Prague	0.111	0.410	0.396	-0.048	0.087	-0.082	-+-	-0.025
ESZ	Esztergom	0.111	0.000	0.908	-0.048	-0.323	0.430	--+	+0.034
WIE	Vienna	0.111	0.000	0.287	-0.048	-0.323	-0.191	---	-0.324
RGB	Regensburg	0.125	0.727	0.367	-0.034	0.404	-0.111	-+-	+0.149
KOL	Cologne	0.125	0.700	0.604	-0.034	0.377	0.126	+++	+0.271
STR	Strasbourg	0.143	0.571	0.158	-0.016	0.248	-0.320	-+-	-0.051
DUB	Dublin	0.125	0.000	0.900	-0.034	-0.323	0.422	--+	+0.038
OXF	Oxford	0.125	0.000	0.333	-0.034	-0.323	-0.145	---	-0.290
CAM	Cambridge	0.125	0.000	0.458	-0.034	-0.323	-0.020	---	-0.218
PAR	Paris	0.143	0.812	0.104	-0.016	0.489	-0.374	-+-	+0.082
ANG	Angers	0.143	0.000	0.567	-0.016	-0.323	0.089	--+	-0.145
DIJ	Dijon	0.167	0.571	0.225	0.008	0.248	-0.253	++-	+0.002
AVI	Avignon	0.167	0.000	0.246	0.008	-0.323	-0.232	+--	-0.316
MON	Montpellier	0.167	0.000	0.408	0.008	-0.323	-0.070	+--	-0.222
TOU	Toulouse	0.143	0.250	0.492	-0.016	-0.073	0.014	--+	-0.043
LIS	Lisbon	0.111	0.000	0.712	-0.048	-0.323	0.234	--+	-0.079
SAL	Salamanca	0.111	0.000	0.483	-0.048	-0.323	0.005	--+	-0.211
SEV	Seville	0.111	0.000	0.479	-0.048	-0.323	0.001	--+	-0.214
VAL	Valencia	0.125	0.571	0.458	-0.034	0.248	-0.020	-+-	+0.112
AST	Asti	0.200	0.750	0.658	0.041	0.427	0.180	+++	+0.374
MIL	Milan	0.200	0.000	0.546	0.041	-0.323	0.068	++-	-0.124
GEN	Genoa	0.200	0.000	0.283	0.041	-0.323	-0.195	+--	-0.275
PIS	Pisa	0.250	0.727	0.650	0.091	0.404	0.172	+++	+0.385
BOL	Bologna	0.250	0.400	0.271	0.091	0.077	-0.207	++-	-0.023
PAD	Padua	0.250	0.000	0.458	0.091	-0.323	-0.020	+--	-0.145
VEN	Venice	0.250	0.000	0.671	0.091	-0.323	0.193	++-	-0.023
RIM	Rimini	0.333	0.625	0.542	0.174	0.302	0.064	+++	+0.312
FIR	Florence	0.250	0.250	0.083	0.091	-0.073	-0.395	+--	-0.217
SIE	Siena	0.250	0.400	0.333	0.091	0.077	-0.145	++-	+0.013
PER	Perugia	0.200	0.400	0.317	0.041	0.077	-0.161	++-	-0.025
ASS	Assisi	0.167	0.625	0.271	0.008	0.302	-0.207	++-	+0.059
TOD	Todi	0.167	0.400	0.250	0.008	0.077	-0.228	++-	-0.083
ROM	Rome	0.167	0.823	0.958	0.008	0.500	0.480	+++	+0.570
ASC	Ascoli	0.143	0.400	0.416	-0.016	0.077	-0.062	-+-	-0.001
CHI	Chieti	0.143	0.812	0.250	-0.016	0.489	-0.228	-+-	+0.141
DJU	Djurazci	0.125	0.000	0.896	-0.034	-0.323	0.418	--+	+0.035
CIV	Civita	0.125	0.727	0.150	-0.034	0.404	-0.328	-+-	+0.024
BAR	Barletta	0.125	0.571	0.800	-0.034	0.248	0.322	-++	+0.309
NAP	Napoli	0.125	0.700	0.683	-0.034	0.377	0.205	-++	+0.317
REG	Reggio	0.125	0.000	0.604	-0.034	-0.323	0.126	--+	-0.133
PAL	Palermo	0.143	0.000	0.583	-0.016	-0.323	0.105	--+	-0.135

References

1. Bailey, N.T.J.: *The Mathematical Theory of Epidemics*. Charles Griffin, London (1957)
2. Baronchelli, A., Pastor-Satorras, R.: Diffusive dynamics on weighted networks. Preprint: arXiv: 0907.3810v1 (2009) [cond-mat.stat.mech]
3. Blau, P.: *Inequality and Heterogeneity*. The Free Press, New York (1977)
4. Castellano, C., Fortunato, S., Loreto, V.: Statistical physics of social dynamics. *Rev. Mod. Phys.* **81** 591 (2009). Preprint: arXiv:0710.3256v1 [physics.soc-ph]
5. Cavalli-Sforza, L.L., Feldman, M.W.: *Cultural Transmission and Evolution: A Quantitative Approach*. Princeton University Press, Princeton (1981)
6. Coleman, J.S., Katz, E., Menzel, H.: The diffusion of an innovation among physicians. *Sociometry* **20** 253–270 (1957)
7. Cowan, R., Jonard, N.: *Network Structure and the Diffusion of Knowledge*. MERIT Technical report 99028, Maastricht University (1999)
8. Degenne, A., Forsé, M.: *Introducing Social Networks*. Sage Publications, London (1999)
9. Doran, J.E. and Gilbert, G.N. (eds.) *Simulating Societies: The Computer Simulation of Social Phenomena*. UCL Press, London (1994)
10. Doreian, P.: Mapping networks through time. In: Weesie, J. and Flap, H. (eds.) *Social Networks through Time*, pp. 245–264. ISOR/University of Utrecht (1990)
11. Fararo, T.J.: Biased networks and social structure theorems. *Social Networks* **3** 137–159 (1981)
12. Granovetter, M.S.: The strength of weak ties. *Am. Journal Soc.* **78** 1360–1380 (1973)
13. Granovetter, M.S.: Threshold models of collective behavior. *Am. Journal Soc.* **83** 1420–1443 (1978)
14. Granovetter, M.S., Soong, R.: Threshold models of diffusion and collective behavior. *Journal Math. Soc.* **9** 165–179 (1983)
15. Guardiola, X., Diaz-Guilera, A., Prez, C.J., Arenas, A., Llas, M.: Modelling diffusion of innovations in a social network. *Phys. Rev. E* **66** 0206121 (2002)
16. Hägerstrand, T.: A Monte Carlo approach to diffusion. *Eur. Journal Soc.* **6** 43–67 (1965)
17. Hegselmann, R., Mueller, U., Troitzsch, K.G. (eds.) *Modelling and Simulation in the Social Sciences from the Philosophy of Science Point of View*. Kluwer Academic Publishers, Dordrecht (1996)
18. Iribarren, J.L., Moro, E.: Information diffusion epidemics in social networks. Preprint: arXiv: 0706.0641v1 (2008) [physics.soc-ph]
19. Kendall, D.G.: *Mathematical Models of the Spread of Infection*. Medical Research Council, London (1965)
20. Marey, E.J.: Les eaux contaminées et le choléra. *CRAS* **99** 667–683 (1884)
21. Moreno, Y., Pastor-Satorras, R., Vespignani, A.: Epidemic outbreaks in complex heterogeneous networks. *Eur. Phys. Journal B* **26** 521–529 (2002)
22. Newman, M.E.J.: The spread of epidemic disease on networks. *Phys. Rev. E* **66** 016128 (2002)
23. Oliver, P.E., Marwell, G., Teixeira, R.: A theory of critical mass, I. Interdependence, group heterogeneity, and the production of collective action. *Am. Journal Soc.* **91** 522–556 (1985)
24. Rapoport, A., Yuan, Y.: Some experimental aspects of epidemics and social nets. In: Kochen, M. (ed.) *The Small World*, pp. 327–348. Ablex Publishing Company, Norwood (1989)
25. Raynaud, D.: *Etudes d'épistémologie et de sociologie des sciences, 2. Pourquoi la perspective a-t-elle été inventée en Italie centrale? Habilitation à diriger les recherches*. Université de Paris Sorbonne, Paris (2004)
26. Rogers, E.M.: Network analysis of the diffusion of innovations. In: Holland, P.W. and Leinhardt, S. (eds.) *Perspectives on Social Network Research*, pp. 137–164. Academic Press, New York (1979)
27. Rogers, E.M.: *Diffusion of Innovations* [1962]. The Free Press, New York (1995)
28. Rogers, E.M., Ascroft, J.R., Röling, N.: *Diffusion of Innovation in Brazil, Nigeria, and India*. Unpublished Report. Michigan State University, East Lansing (1970)

29. Rogers, E.M., Kincaid, D.L.: *Communication Networks: Towards a New Paradigm for Research*. The Free Press, New York (1981)
30. Simonsen, I., Eriksen, K.A., Maslov, S., Sneppen, K.: Diffusion on complex networks: a way to probe their large-scale topological structures. *Physica A* **336** 163–173 (2004)
31. Simonsen, I.: Diffusion and networks: a powerful combination. *Physica A* **357** 317–330 (2005)
32. Skillnäs, N.: Modified innovation diffusion. A way to explain the diffusion of cholera in Linköping in 1866. A study of methods. *Geografiska Annaler B: Human Geography* **81** 243–260 (1999)
33. Skvoretz, J.: Salience, heterogeneity, and consolidation of parameters: civilizing Blaus primitive theory. *American Sociological Review* **48** 360–375 (1983).
34. Stauffer D., Solomon, S.: Physics and mathematics applications in social science. In: Mayers, R.A. (ed): *Encyclopedia of Complexity and Systems Science*. Springer, New York, pp. 6804–6810 (2009). Preprint: arXiv:0801.01121v1 [physics.soc-ph]
35. Valente, T.W.: *Network Models of the Diffusion of Innovations*. Hampton Press, Creskill (1995)
36. Valente, T.W.: Social network thresholds in the diffusion of innovations. *Social Networks* **18** 69–89 (1996)
37. Valente, T.W.: Network models and methods for studying the diffusion of innovations. In: Carrington, P.T., Scott, J. and Wasserman, S. (eds.) *Models and Methods in Social Network Analysis*, pp. 98–116. Cambridge University Press, New York (2005)
38. Verhulst, P.F.: Notice sur la loi que la population suit dans son accroissement. *Corresp. math. phys.* **4** 113–121 (1838)
39. Watts, D.J., Strogatz S.H.: Collective dynamics of small world networks. *Nature* **393** 440–442 (1998)

Credits

“All figures are property of the author, except fig. 2, reprinted with permission of Hampton Press.”